



Universiteit
Leiden
The Netherlands

Pre-implantation and placental development in humans and mice

He, N.

Citation

He, N. (2017, October 24). *Pre-implantation and placental development in humans and mice*. Retrieved from <https://hdl.handle.net/1887/58876>

Version: Not Applicable (or Unknown)

License: [Licence agreement concerning inclusion of doctoral thesis in the Institutional Repository of the University of Leiden](#)

Downloaded from: <https://hdl.handle.net/1887/58876>

Note: To cite this publication please use the final published version (if applicable).

Cover Page



Universiteit Leiden



The following handle holds various files of this Leiden University dissertation:
<http://hdl.handle.net/1887/58876>

Author: He, N.

Title: Pre-implantation and placental development in humans and mice

Issue Date: 2017-10-24

CHAPTER 6

At term, XmO and XpO mouse placentas show differences in glucose metabolism in the trophoderm-derived outer zone

Nannan He¹, Shujing Jane Lim^{1,#}, Joana C. Moreira de Mello², Injerreau Navarro¹, Monika Bialecka¹, Daniela C. F. Salvatori^{1,3}, Lucette A. J. van der Westerlaken⁴, Lygia V. Pereira^{2,5}, Susana M. Chuva de Sousa Lopes^{1,5,¶}

¹Department of Anatomy and Embryology, Leiden University Medical Center, Leiden, The Netherlands

²Department of Genetics and Evolutionary Biology, University of São Paulo, São Paulo, Brazil

³Central Laboratory Animal Facility, Leiden University Medical Center, Leiden, The Netherlands

⁴Department of Gynaecology, Leiden University Medical Center, Leiden, The Netherlands

⁵Department for Reproductive Medicine, Ghent University Hospital, Ghent, Belgium

[#]Current address: University of Edinburgh, College of Medicine and Veterinary Medicine, Edinburgh, United Kingdom

[¶]Equal senior authorship contribution

Frontiers in Cell and Developmental Biology 2017, 5(63).

ABSTRACT

Genetic mouse model (39,XO) for human Turner syndrome (45,XO) harboring either a single maternally inherited (Xm) or paternally inherited (Xp) chromosome show a pronounced difference in survival rate at term. However, a detailed comparison of XmO and XpO placentas to explain this difference is lacking. We aimed to investigate the morphological and molecular differences between XmO and XpO term mouse placentas. We observed that XpO placentas at term contained a significantly larger area of glycogen cells (GCs) in their outer zone, compared to XmO, XX and XY placentas. In addition, the outer zone of XpO placentas showed higher expression levels of lactate dehydrogenase (*Ldha*) than XmO, XX and XY placentas, suggestive of increased anaerobic glycolysis. In the labyrinth, we detected significantly lower expression level of trophoctoderm (TE)-marker keratin 19 (*Krt19*) in XpO placentas than in XX placentas. The expression of other TE-markers was comparable as well as the area of TE-derived cells between XO and wild-type labyrinths. XpO placentas exhibited specific defects in the amount of GCs and glucose metabolism in the outer zone, suggestive of increased anaerobic glycolysis, as a consequence of having inherited a single Xp chromosome. In conclusion, the XpO genotype results in a more severe placental phenotype at term, with distinct abnormalities regarding glucose metabolism in the outer zone.

INTRODUCTION

Turner syndrome is the most common sex chromosome disorder affecting 1 in 2000 live births. It is caused by the loss of genetic material from one of the sex chromosomes and the retained single X chromosome can be inherited either from the mother (Xm) or the father (Xp) [1]. In humans, 99% of the XO fetuses are lost during pregnancy [2, 3]. By contrast, in mice, 90% of embryos with a single Xm survive to term, whereas 40% of embryos with a single Xp are resorbed due to severe placental abnormalities [4-6]. This suggests that the transcription of a single Xm or Xp in mouse placentas is not equivalent and influences development differently, reflecting either a different genome-wide epigenetic landscape between Xp and Xm or the existence of certain paternally imprinted X-linked genes in the mouse placenta.

X chromosome inactivation (XCI) is better understood in mice than in humans [7-11] due to the existence of well-studied genetic substrains of mice. In mice, in female (XX) late blastocysts, the trophectoderm (TE) and primitive endoderm (PE) show imprinted XCI (with an obligatory active Xm) and the epiblast (EPI) shows random XCI (in each cell either the Xm or Xp is active) [7, 10, 12]. In the placenta, the TE-derived cells [trophoblast giant cells (TGCs), spongiotrophoblasts and glycogen cells (GCs) in the outer zone; mononuclear trophoblast cells and syncytiotrophoblast cells in the labyrinth] maintain imprinted XCI (active Xm). By contrast, the chorionic plate and the embryonic endothelial cells of the labyrinth are derived from EPI, therefore showing random XCI.

In humans, there may not be imprinted XCI in the placenta [13-15]. In agreement, by the end of the first trimester, the placental volume between XO and control placenta seemed comparable [16] and the birth weight of XmO and XpO new-born babies was similar [17]. Nevertheless, there is a higher incidence of XpO human fetuses lost during pregnancy [18] and the percentage of patients retaining the XmO is 60%-80% [19-23].

The placenta is a crucial organ during mammalian development, ensuring the selective and directional transport of gases, nutrients and waste products between the maternal blood and the embryonic blood [24]. In mice, the GCs may serve as a potential additional energy source, due to their high glycogen content and sensitivity to glucagon signaling [25]. The placenta is a highly regulative organ that adapts constantly to the maternal environment, for example oxygen tension and hypoxia [26, 27], availability of nutrients or calorie restriction [28] and exposure to maternal hormones [29, 30] to sustain optimal embryonic growth throughout pregnancy.

Interestingly, (epi)genetic abnormalities that affect placental development trigger an adaptive response in the placenta to suppress the decreased efficiency to support embryonic growth [31-34]. In the case of XO embryos, embryonic day (E)8.5 XpO embryos had been shown to have small ectoplacental cones [35]. However, by E14, XpO placentas had caught up in size and some showed a larger outer zone [36]. At E18.5, XpO placentas were significantly heavier than XX controls [5]. But in a later study, XmO, XpO and XY placentas were found heavier than XX placentas [37].

To date, a detailed comparison of XmO and XpO term placentas, in particular the TE-derived part of the placenta, is missing. Here, we show that E18.5 XpO placentas exhibited significantly larger area occupied by GCs in outer zone when compared to XmO, XX and XY placentas. Moreover, the expression of *Ldha*, coding for the enzyme that converts lactate to pyruvate through anaerobic glycolysis, was significantly higher in outer zone of XpO placentas than the XmO, XX and XY placentas, suggesting increased anaerobic glycolysis and underlying possible defects in oxygen availability in XpO placentas. In conclusion, the XpO genotype results in a more severe placental phenotype at term, with distinct abnormalities regarding glucose metabolism in the outer zone.

MATERIALS AND METHODS

Mice and genotyping

All animal tissues used in this work were a generous gift from P. Burgoyne in accordance with the United Kingdom Animals Scientific Procedures Act 1986 and approved by the local ethical committee of the National Institute of Medical Research, London. MF1 mice bearing XX and XY embryos were from XX x XY crossings. XmO and XpO mice were generated as previously described [37]. Briefly, XmO animals were produced by crossing XX females with XYO males, and identified by visual detection of female genitalia; the XYO males were generated by crossing XPafO females with XY* males. The XpO animals were generated by crossing In(X) Paf/X females with XY males. All females (In(X)/X, XXPaf and XpO) were karyotyped with trypsin-Giemsa banding using fresh liver to identify the XpO embryos (with 39 chromosomes as opposed to 40 chromosomes).

Placenta collection and histology

From a total of 12 litters, E18.5 embryos were isolated in phosphate buffer saline (PBS) and separated into males and females by morphology and genotyped as above. The placentas were dissected into quarters and some quarters were collected for RNA isolation after removal of the outer zone (Jz, TGCs and decidua), whereas others were fixed in 4% paraformaldehyde (PFA, Merck, Darmstadt, Germany) at 4°C overnight (o/n), washed in PBS and dehydrated through increasing concentrations of ethanol and finally xylene, embedded in paraffin and serially sectioned (5 µm) in the sagittal plane using a microtome (Leica RM2055, Nussloch, Germany) in the medial-to-lateral direction (N=3 XX, N=3 XY, N=5 XmO, N=4 XpO).

Prior to Periodic acid-Schiff (PAS) staining, sections were deparaffinised in xylene, rehydrated through a series of ethanol solutions and incubated 30 minutes at 56°C in pre-heated 1% periodic acid (Sigma-Aldrich, St. Louis, USA), rinsed in water, immersed in Schiff's reagent (Klinipath, Duiven, The Netherlands) 30 minutes at room temperature (RT), rinsed in water and counterstained with Mayer's haematoxylin (Merck, Darmstadt, Germany). Congo red, Masson's trichrome and Hematoxylin-eosin staining were performed using standard histological procedures. Stained sections were washed in water, dehydrated through a series of ethanol, xylene and mounted in Entellan (Merck, Darmstadt, Germany).

Quantitative reverse-transcription polymerase chain reaction (QPCR)

QPCR was performed on placental quarters after removal of the outer zone and analyzed as described [38]; or on RNA material isolated from 5x paraffin sections of the outer zone using RecoverAll total nucleic acid isolation kit (AM1975, Ambion, Carlsbad, CA, USA) following the manufacturer's protocol. For normalization, the $\Delta\Delta\text{Ct}$ method was used with the reference genes *Ubc* and *B2m*, stably expressed in mouse placenta [39]. All individual placentas were analysed in technical triplicates. The fold change in expression was calculated relative to the XX1 placenta. Briefly, the average ΔCt value from the technical triplicates of the XX1 (Ave ΔCt XX1) was calculated. Next, we subtracted Ave ΔCt XX1 from each ΔCt ($\Delta\Delta\text{Ct}$) and the relative fold change ($2^{-(\Delta\Delta\text{Ct})}$) calculated. The fold change of each of the triplicate values per placenta was then averaged (mean) and the standard deviation was calculated. The primers used are listed in S1 Table.

Immunofluorescence

Paraffin sections were deparaffinised and used for immunofluorescence as previously described [40]. Primary antibodies used were rabbit anti-KRT19 (or keratin 19) (1:250; ab52625, Abcam, Cambridge, UK) and rat anti-EMCN (or endomucin) (1:150; sc-65495, Santa Cruz Biotechnology, Santa Cruz, CA, USA). Afterwards, sections were washed in 0.05% Tween-20/PBS, treated with 0.3% Sudan Black B (Edward Gurr Ltd, London, UK) in 70% ethanol for 5 minutes to eliminate background autofluorescence from red blood cells [41] and incubated with secondary antibodies diluted in blocking solution for 1 hour at RT. Secondary antibodies were Alexa Fluor 488 goat anti-rabbit (1:500; A-11034, Life Technologies, Eugene, OR, USA) and Alexa Fluor 555 goat anti-rat (1:500; A-21434, Life Technologies, Eugene, OR, USA). Nuclei were stained with 4',6-diamidino-2-phenylindole (DAPI) (Vector Laboratories, Peterborough, UK) and sections were mounted in Prolong Gold anti-fade reagent (Life technologies, Eugene, OR, USA). Slides used for isotype controls were treated as above using rabbit immunoglobulin fraction (1:250; X0903, Dako, Heverlee, Belgium) and rat IgG2a (1:150, MAB006, R&D Systems, Minneapolis, MN, USA) instead of the primary antibodies.

Imaging and quantification

Bright-field images were taken on an Olympus AX70 microscope (Olympus, Zoeterwoude, Netherlands) equipped with a digital camera (Olympus XC50, Tokyo, Japan). Fluorescence images were acquired on a Leica DMRA fluorescence microscope (Leica, Wetzlar, Germany) with a CoolSnap HQ2 camera (Photometrics, Tucson, USA) or a Leica AF6000 fluorescence microscope with a Hamamatsu EM-CCD C9100 camera (Leica Microsystems, Wetzlar, Germany). Quantification was performed in ImageJ 1.48 (<http://imagej.nih.gov/ij>).

Statistical analysis

The statistical analyses of the proportion of glycogen cells area in the outer zone of the placentas, the percentage of fetal vascular space, the area occupied by TE-derived cells in the

labyrinth and differential gene expression per genotype were performed using one-way ANOVA with the Tukey-HSD applied for post hoc testing, using statistical software package SPSS 20.0 (SPSS Inc., Chicago, IL, USA). $P < 0.05$ was considered significant.

RESULTS

At term, XpO placentas showed larger area occupied by GCs in the outer zone

We investigated the placental morphology of the four genotypes (N=3 XX, N=3 XY, N=5 XmO, N=3 XpO) at E18.5 using PAS-staining. This allowed us to distinguish the outer zone from the labyrinth (Fig 1A). We observed the presence of a broader outer zone in the lateral part of XmO (N=2 in 5, 40%) and XpO (N=3 in 3, 100%) placentas (Fig 1A). To quantify the area occupied by GCs in the outer zone, the ratio of the area occupied by GCs in the outer zone was calculated on individual placental sections (n=3-5 medial sections per placenta, containing a visible connection to the umbilical cord) (Fig 1B-C). The XpO placentas contained a significantly larger area occupied by GCs in the outer zone when compared to XX, XY and XmO placentas ($P=0.004$, 0.008 and 0.045 respectively, Fig 1C). In contrast, the area occupied by GCs in the outer zone of XmO placentas was comparable to that of XX and XY placentas (Fig 1C).

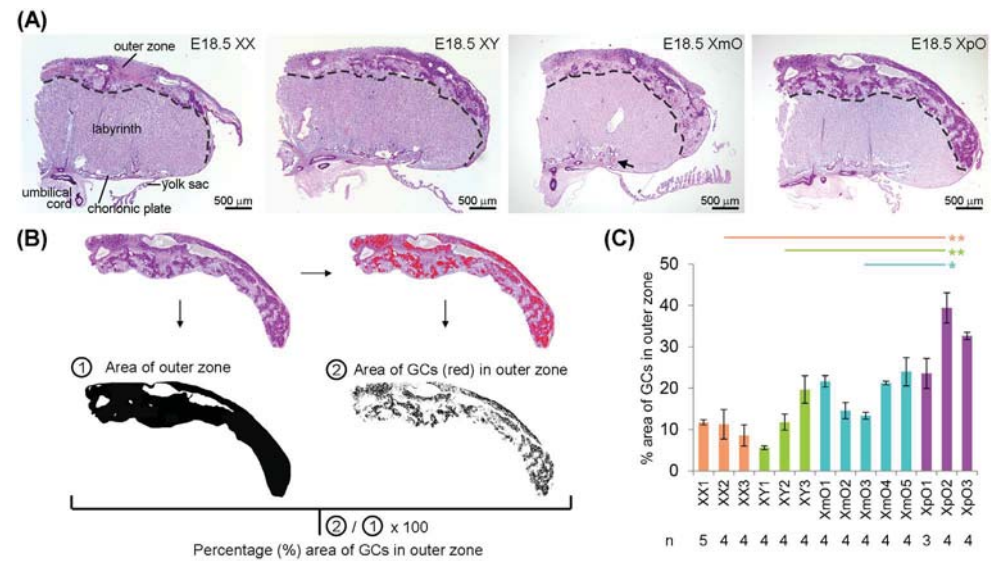


Fig 1. XpO placentas have a larger area occupied by glycogen cells in the outer zone.

(A) Representative PAS-stained medial placental sections of the different genotypes (XX, XY, XmO, XpO). (B) From the images acquired by microscopy, the outer zone of the placenta is digitally selected, then converted to black-and-white on ImageJ to provide the total area of the outer zone. From the selected outer zone of the placenta, the dark PAS-stained glycogen cells (GCs) are identified digitally (red cells) by selecting a threshold on Image J. The percentage of the GCs in the outer zone of each placenta section is obtained by using the ratio of the area of GCs ②/total area of the outer zone ①. (C) Graph depicting the percentage (%) area of outer zone occupied by GCs in the different genotypes (XX, XY, XmO, XpO). Significant P values between XpO placentas and the other genotypes are indicated by * ($P < 0.05$) and ** ($P < 0.01$).

At term, XpO placentas showed increased *Ldha* expression in the outer zone

The larger area of GCs in outer zone of XpO placentas led us to investigate defects in gene expression related to glucagon signaling and glucose metabolism (Fig 2A) in the outer zone. The expression level of glucagon receptor (*Gcgr*) as well as of glucose transporter *Slc2a1*, which mediate passive glucose uptake in cells [42] was similar between XmO, XpO and XX placentas (Fig 2B, S2 Table).

Two X-linked genes, *G6pdx* and *Pgk1*, encode essential enzymes in the conversion of glucose to pyruvate [43, 44]. In the outer zone, *G6pdx* showed significantly lower expression in both XmO and XpO placentas compared to the XX placentas (XmO versus XX: $P=0.028$; XpO versus XX: $P=0.007$; Fig 2B, S2 Table). However, expression of *Pgk1* was significantly higher in XpO placentas than in XmO placentas ($P=0.009$, Fig 2B, S2 Table).

Under normal oxygen supply (aerobic glycolysis), pyruvate is catabolized into acetyl-CoA to be used in the tricarboxylic acid (TCA) cycle to produce energy efficiently (Fig 2A). One of the enzymes of the TCA cycle, encoded by X-linked gene *Idh3g*, showed similar expression between XO and wild-type placentas (Fig 2B, S2 Table). However, if oxygen supply is low, pyruvate is metabolized to lactate (anaerobic glycolysis). In anaerobic glycolysis, the key

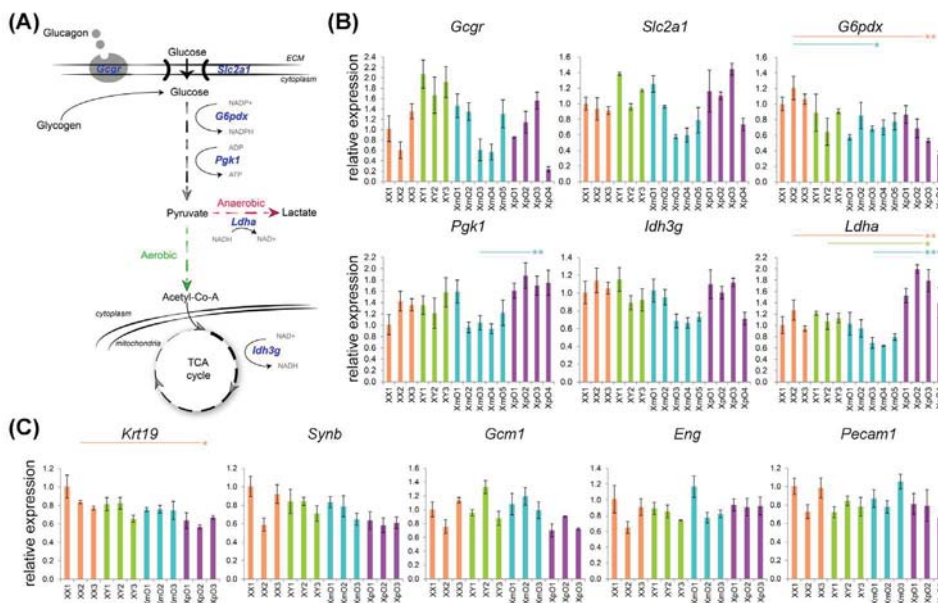


Fig 2. Expression of genes related to glucose metabolism in the outer zone and expression of genes related to TE and vasculature in the labyrinth.

(A) Scheme of glucose metabolism cascade, with the genes analyzed in blue. (B) Relative expression of the depicted genes in the outer zone of XX, XY, XmO, XpO placentas. Each bar represents mean \pm standard deviation of technical triplicates of a different placenta. Significant P values between genotypes are indicated by * ($P < 0.05$), ** ($P < 0.01$) and *** ($P < 0.001$). (C) Relative expression of the depicted genes in the labyrinth of XX, XY, XmO, XpO placentas. Each bar represents mean \pm standard deviation of technical triplicates of a different placenta. Significant P value between XX and XpO is indicated by * ($P < 0.05$).

enzyme that converts pyruvate into lactate is encoded by the *Ldha* gene. The expression levels of *Ldha* in the outer zone of XpO placentas were significantly higher than in the other placentas (XpO versus XX: $P=0.007$; XpO versus XY: $P=0.015$; XpO versus XmO: $P<0.001$; Fig 2B, S2 Table), suggesting higher levels of anaerobic respiration specifically in the outer zone of the XpO placentas, where a higher incidence of GCs was found.

The labyrinths of XO and wild-type placentas were comparable

Next, we determined the relative expression of TE markers [keratin 19 (*Krt19*), syncytin b (*Symb*), glial cells missing homolog 1 (*Gcm1*)] and endothelial markers [endoglin (*Eng*), platelet/endothelial cell adhesion molecule 1 (*Pecam1*)] in the labyrinth of the four types of placentas.

The expression levels of TE-marker *Krt19* in the labyrinth of XpO placenta were significantly lower than that in XX placenta ($P=0.024$, Fig 2C, S2 Table). However, the TE-markers *Symb* and *Gcm1* were similarly expressed in the four types of placentas (Fig 2C, S2 Table). There was also no difference in the expression of endothelial-markers *Eng* and *Pecam1* in the labyrinth (Fig 2C, S2 Table). Together, the data suggests that the labyrinth of XO placentas may be similar to wild-type placentas.

To further confirm that, we quantified the area occupied by (EMCN-positive) fetal capillaries and (KRT19-positive) TE-derived cells in the labyrinth (n=3-5 sections per individual placenta; N=3 XX, N=3 XY, N=5 XmO, N=4 XpO) (Fig 3). For the quantification, single channel images of the labyrinth zone from medial placental sections immunostained for anti-EMCN (red) and anti-KRT19 (green) and DAPI (details shown in Fig 3B,D,E) were used. The area of the fetal vasculature (Fig 3B), considered the area occupied by the EMCN-positive fetal capillaries, was similar between XO and wild-type labyrinths (Fig 3C, left panel). Moreover, the vascular density, calculated as the number of fetal capillaries per image, was also comparable between XO and wild-type labyrinths (Fig 3C, right panel).

To quantify the area of occupied by TE-derived cells, the nuclei area (DAPI-positive) was merged with the KRT19-positive cytoplasmic staining of the TE derived cells. However, to exclude the nuclear area of the fetal vasculature, we subtracted the fetal vascular area (Fig 3B,D,E). In this way, we obtained the area occupied solely by TE-derived cells (cytoplasm and nuclei). We concluded that the area occupied by TE-derived cells in labyrinth was similar between XO and wild-type placentas (Fig 3E).

At term, XpO placentas showed decreased *Xlr4b/4c* in the labyrinth zone

The X-linked *Xlr3b* has previously been identified as differentially expressed in XmO and XpO brains, but not in the placentas [45]. In addition to *Xlr3b*, *Xlr4b/4c* were also reported to be differentially expressed between XmO and XpO brains, but at least *Xlr4c* not in placentas [46]. However, whole placentas were used for analysis and a possible regional regulation could have been missed. We therefore investigated the expression of *Xlr3b* and *Xlr4b/4c* separately in outer zone and labyrinth zone of term placenta.

We did not observe significantly differential expression of *Xlr3b* and *Xlr4b/4c* in the XpO and XmO outer zones (Fig 4A, S2 Table), even though XpO outer zones had significantly lower *Xlr3b* than XY outer zones ($P=0.030$; Fig 4A, S2 Table). In the labyrinth zone, the expression levels of *Xlr3b* were comparable between genotypes (Fig 4B, S2 Table), but surprisingly XpO labyrinth zone had significantly lower expression levels of *Xlr4b/4c* than the other placentas (XpO versus XX: $P=0.006$; XpO versus XY: $P<0.001$; XpO versus XmO: $P=0.003$; Fig 4B, S2 Table).

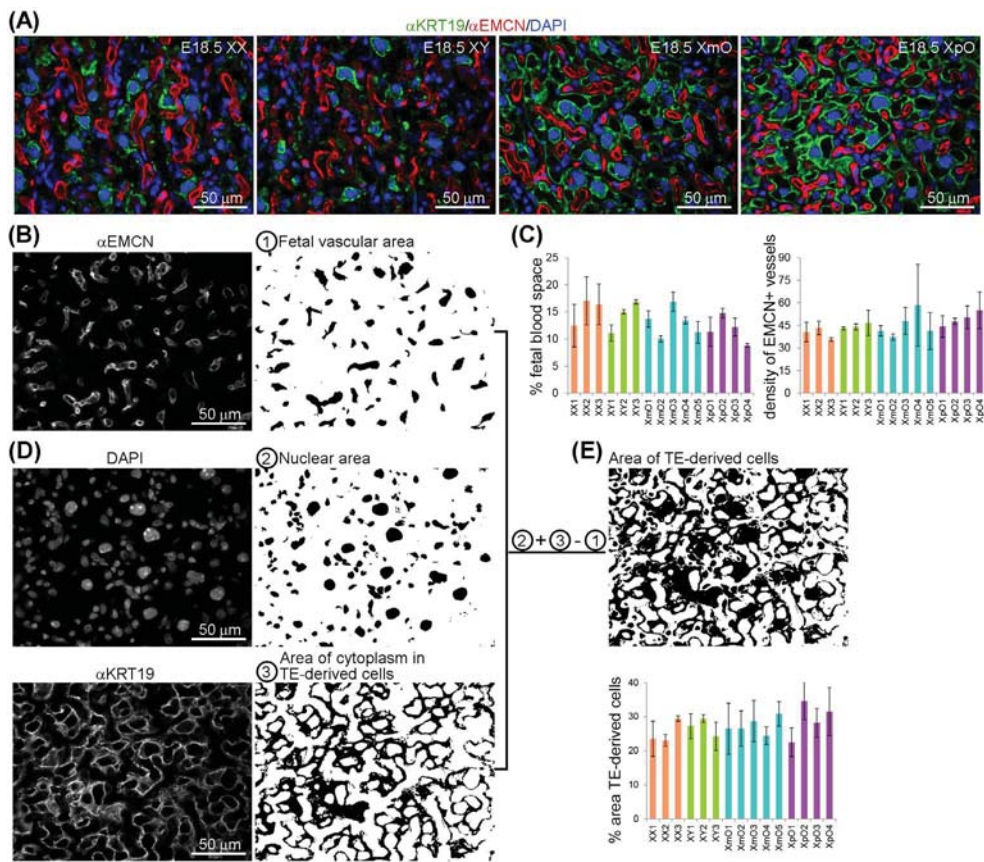


Fig 3. XO placentas show comparable fetal vascular area and TE-derived cell area in the labyrinth.

(A) Representative medial placental sections from the different genotypes (XX, XY, XmO, XpO) immunostained for KRT19 and EMCN show the organization of the fetal vasculature and maternal blood space in the labyrinth. (B) To quantify the fetal vascular area and density, single channel images for EMCN-positive fetal capillaries are filled with black area ① and either the number of vessels counted (density of fetal vessels in that area) or the percentage of fetal vascular area is quantified (sum of the area of EMCN-positive blood vessels/total area of the image x 100). (C) Graph depicting the percentage (%) of area occupied by fetal vasculature and the density of EMCN-positive fetal blood vessels in the different genotypes analyzed (XX, XY, XmO, XpO). (D) To calculate the percentage of area occupied by TE-derived cells, the single channel images for DAPI ② and KRT19 ③ are converted to black-and-white, added digitally and finally from that area (②+③) the fetal capillary area is subtracted (②+③-①) (sum of the resulting black area/total area of the image x 100). (E) Graph depicts the percentage (%) of area occupied by TE-derived cells in the different genotypes analyzed (XX, XY, XmO, XpO).

At term, XmO placentas contained higher incidence of fibrin nodules in the maternal arterial sinuses adjacent to the chorionic plate

Interestingly, the XmO placentas contained small nodules, partially occluding some maternal arterial sinuses proximal of the chorionic plate (black arrow in Fig 1A). After Congo red, Masson's trichrome and Hematoxylin-eosin staining, we concluded that those were fibrin deposits (Fig 5A).

To quantify the incidence of fibrin nodules in the different placentas (N=3 XX, N=3 XY, N=5 XmO, N=4 XpO), we manually counted the number of fibrin nodules present in medial placental sections. All XmO placentas contain fibrin deposits in most sections analyzed, whereas the nodules were not observed in most of the other placentas (XmO versus XX: $P=0.0007$; XmO versus XY: $P=0.0007$; XmO versus XpO: $P=0.0019$; Fig 5B). On average, per section one or two nodules were observed (Fig 5A,C).

DISCUSSION

The lack of a second sex chromosome in XO mouse embryos leads to the development of smaller trophoblast ectoplacental cones and, in some cases, pregnancy loss [5, 6, 35, 37, 47]. Our study on XO placental abnormalities in mice shows that inheriting the single X chromosome from the paternal or maternal side leads to different placental phenotypes: E18.5 XpO placentas contained a larger area of GCs in the outer zone with a possible consequent increase in anaerobic glycolysis and/or oxygen availability. This does not seem to be the case in XmO placentas. By contrast, XmO placentas show increased incidence of small fibrin nodules in maternal arterial sinuses proximal of the chorionic plate.

The placenta is sensitive to defects in epigenetic regulation, such as regulation of imprinted genes and imprinted X inactivation [31-33]. As such, it is not surprising that many imprinted and X-linked genes are expressed in the placenta and regulate metabolism and growth [31, 33, 34]. Defects in the epigenetic regulation of imprinted regions/genes often result in expansion

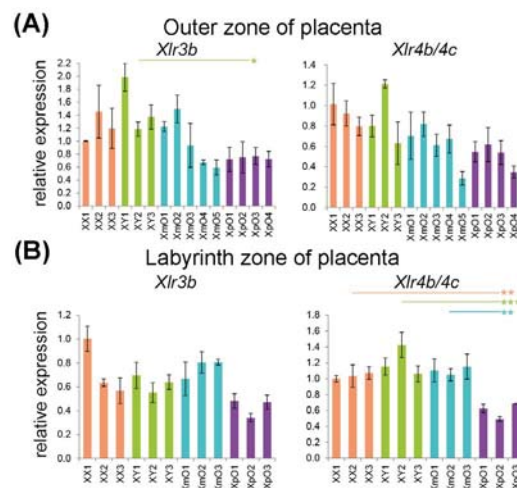


Fig 4. *Xlr* genes expression in the outer zone and labyrinth zone of term placentas.

(A-B) Relative expression of *Xlr3b* and *Xlr4b/4c* in the outer zone (A) and labyrinth zone (B) of XX, XY, XmO, XpO placentas. Each bar represents mean \pm standard deviation of technical triplicates of a single placenta. Significant P values between genotypes are indicated by * ($P<0.05$), ** ($P<0.01$) and *** ($P<0.001$).

of the outer zone of the placenta [31, 33, 34]. The higher incidence of GCs in the outer zone of XpO placentas may be such an adaptive response to placental insufficiency. Studies in mice show that XpO fetuses have a higher risk of being lost during pregnancy, whereas XmO fetuses generally have a better chance of surviving to term [6, 35]. In XX fetuses, the Xp is preferentially inactivated in the TE-derived tissues [48]. Thus, in both females and males, it is the Xm that is active in TE-derived tissues during placental development. Epigenetic differences between Xp and Xm, including genome-wide differences in chromatin condensation or the existence of X-linked paternally imprinted genes in the placenta, could explain why XpO embryos have a higher risk of being lost during pregnancy.

Alternatively, as a smaller trophoblast ectoplacental cone in XO embryos is often associated with a delay in embryonic development [35, 37, 47], the alteration observed in GCs in outer zone of XpO placentas could reflect a general small delay in development instead of an (active) adaptive response. Interestingly, it has been shown that both the number of GCs and the

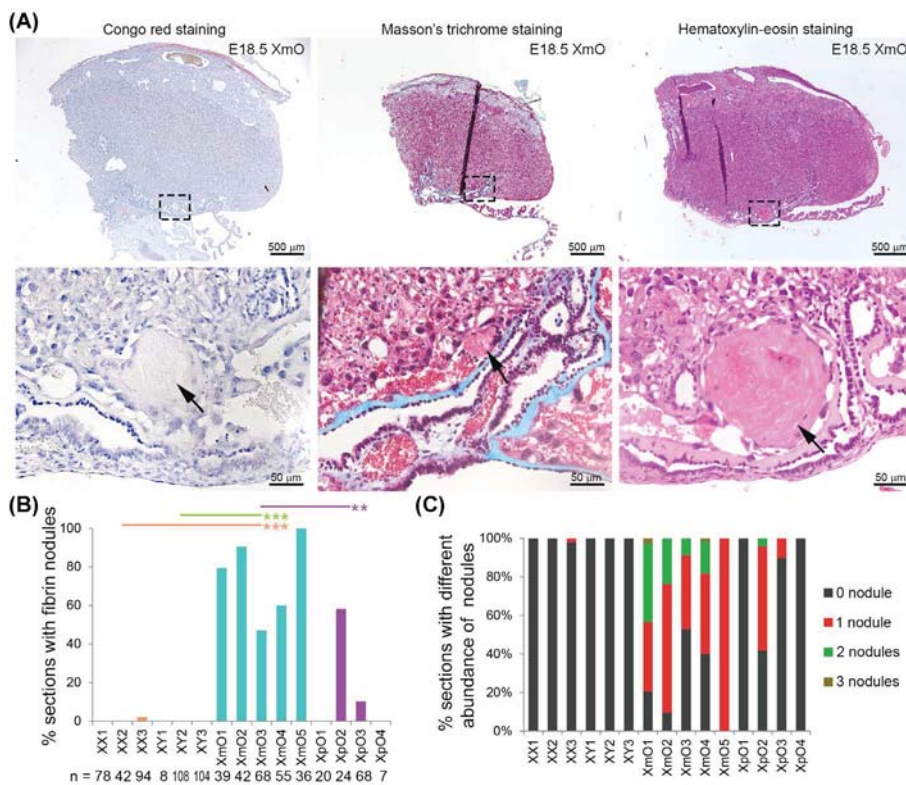


Fig 5. Identifications and quantification of fibrin deposits in term placentas.

(A) Representative medial XmO placenta sections with Congo red, Masson's trichrome and Hematoxylin-Eosin staining. The dashed boxes in top panels are shown as magnification in bottom panels. Black arrows point to fibrin deposits. (B) Graph depicting the percentage (%) of placental sections with fibrin nodules per histological section (n) in different genotypes. Significant *P* values between XmO placentas and the other genotypes are indicated by ** ($P < 0.01$) and *** ($P < 0.001$). (C) Graph depicting the percentage (%) of placental sections with different abundance of fibrin nodules per histological section (n) in different genotypes.

volume of the junctional zone increases during gestation, peaks at E16.5, followed by reduction until birth [25, 49]. Therefore, if the physiological regression of GCs in XpO placentas was delayed, this would result in relatively more GCs and increased size of the outer zone at E18.5 compared to wild-type placentas.

Abnormal GC numbers, related to impaired glucose transport and glycogen metabolism in placenta [50, 51], have been reported in several mutant mouse placentas, including that of X-linked and imprinted genes, and usually result in runting. Opposite phenotypes regarding GCs numbers can still develop in mouse mutants showing a normal placenta at E10.5. As the XpO phenotype, maternally inherited defects in X-linked *Evx1* also showed higher numbers of GCs, spongiotrophoblasts and secondary TGCs by E14.5 and the mutant pups were smaller at birth [52]. By contrast, *Cited2* KO and the imprinted (paternally-expressed) *Igf2* KO mice show severe reduction of numbers of GCs, spongiotrophoblasts and secondary TGCs at E12.5-13.5 [53, 54], but this also resulted in reduced weight at birth [51]; whereas the imprinted (maternally-expressed) *Cdkn1c* (or *p57Kip2*) KO showed placentomegaly, with larger labyrinth zone and excess of spongiotrophoblasts, but normal number of GCs and TGCs and no difference in the weight of embryos [55].

It is unclear whether Xlr factors are directly involved in glucose metabolism, but they could impact on cell differentiation in the outer zone towards GC cells. We observed similar expression of *Xlr3b* and *Xlr4b/4c* in XpO and XmO outer zones suggesting that these genes are not involved in the production of GCs and are not imprinted in the (TE-derived) outer zone. However, the biological significance of the specific decrease in *Xlr4b/4c* in XpO labyrinth remains to be investigated. If this decrease is not due to imprinting in TE-derived labyrinth cells (mononuclear trophoblast and syncytiotrophoblast cells), then perhaps *Xlr4b/4c* could be imprinted and silenced on the Xp in the EPI-derived endothelial cells of the labyrinth, in line with the reported imprint in the brain (Raefski and O'Neill, 2005). This could explain the 40% reduction in expression observed.

Small fibrin nodules, most probably from maternal blood-clots, were observed in the maternal sinus of all XmO placentas, but not in most of the other placentas. Interestingly, TE-derived cells at the fetal-maternal interface in both mouse and human exhibit endothelial-like properties (endovascular extravillous trophoblast cells and syncytiotrophoblast cells in humans; syncytiotrophoblast cells in mice) and seem to be involved in the regulation of coagulation during pregnancy [56]. Fibrin deposits are occasionally described in the labyrinth and spongiotrophoblast area of mouse placentas [57, 58]; and in the perivillous space, associated with local syncytial denudation, in human placentas [59, 60]. Excessive fibrin deposits at the fetal-maternal interface early during development, such as in *Procr* (or *Epcr*) KO embryos results in severe placental thrombosis and lethality at E10.5 [61]; whereas in *Wnt2* KO embryos showed fibrin deposits between E14-18 with maternal blood accumulation in the labyrinth zone, resulting in 50% viability and smaller pups at birth [62]. The fibrin deposits in XmO placentas indicate excessive activation of the coagulation cascade in the maternal circulation, but this obstruction was not as

severe as in *Wnt2* KO mice and, as such, does not seem to be pathological.

In conclusion, mouse embryos with a single Xp have a lower chance than XmO embryos to survive to term due to placental insufficiency. Here, we show that XmO and XpO term placentas differ significantly in the amount of GCs in the outer zone and that XpO placentas may have shifted towards anaerobic glycolysis. This shift in glucose metabolism does not seem to be a direct consequence of altered expression of X-linked genes involved in this metabolism (although *Pgk1* expression differs between XmO and XpO outer zones), but rather a consequence of an altered cellular composition of the XpO outer zone (large GCs area) due to placental adaptive response earlier during development. Our findings highlight the need to investigate glucose metabolism in the placenta of human Turner patients, which may provide individual potential therapeutic strategies for Turner syndrome.

ACKNOWLEDGEMENTS

We would like to express our gratitude to A. Ojarikre, and P. Burgoyne, MRC National Institute for Medical Research, the Ridgeway, Mill Hill, London, UK for the work involved in mouse husbandry, the logistics of the crossings and timed matings and for performing the genotyping/karyotyping of the embryos; L. van Iperen for histology; B. Reinius for isolating RNA; J. Goeman for advise on the statistical test to use and A. Zwijsen and N. Criem for useful discussions.

FUNDING

NH is funded by the China Scholarship Council (CSC) [NO.201307040026]; JCMdM is funded by Fundação de Amparo à Pesquisa do Estado de São Paulo (FAPESP) [2009/17481-6; 2015/03610-0] and LVP by Fundação de Amparo à Pesquisa do Estado de São Paulo (FAPESP) [CEPID 13/08135-2]; SMCdSL is funded by the Interuniversity Attraction Poles-Phase VII, Belgium [IUAP/PAI P7/14].

REFERENCES

1. Saenger P: Turner's syndrome. *N Engl J Med* 1996, 335:1749-1754.
2. Cockwell A, MacKenzie M, Youings S, Jacobs P: A cytogenetic and molecular study of a series of 45,X fetuses and their parents. *J Med Genet* 1991, 28:151-155.
3. Ranke MB, Saenger P: Turner's syndrome. *Lancet* 2001, 358:309-314.
4. Burgoyne PS, Evans EP, Holland K: XO monosomy is associated with reduced birthweight and lowered weight gain in the mouse. *J Reprod Fertil* 1983, 68:381-385.
5. Burgoyne PS, Tam PP, Evans EP: Retarded development of XO conceptuses during early pregnancy in the mouse. *J Reprod Fertil* 1983, 68:387-393.
6. Hunt PA: Survival of XO mouse fetuses: effect of parental origin of the X chromosome or uterine environment? *Development* 1991, 111:1137-1141.
7. Payer B, Lee JT: X chromosome dosage compensation: how mammals keep the balance. *Annu Rev Genet* 2008, 42:733-772.
8. Payer B, Lee JT: Coupling of X-chromosome reactivation with the pluripotent stem cell state. *RNA Biol* 2014, 11:798-807.
9. Petropoulos S, Panula SP, Schell JP, Lanner F: Single-cell RNA sequencing: revealing human pre-implantation development, pluripotency and germline development. *J Intern Med* 2016, 280:252-264.
10. Okamoto I, Patrat C, Thepot D, Peynot N, Fauque P, Daniel N, Diabangouaya P, Wolf JP, Renard JP, Duranthon V, Heard E: Eutherian mammals use diverse strategies to initiate X-chromosome inactivation during development. *Nature* 2011, 472:370-374.
11. Deng X, Berletch JB, Nguyen DK, Distechi CM: X chromosome regulation: diverse patterns in development, tissues and disease. *Nat Rev Genet* 2014, 15:367-378.
12. Silva J, Nichols J, Theunissen TW, Guo G, van Oosten AL, Barrandon O, Wray J, Yamanaka S, Chambers I, Smith A: Nanog is the gateway to the pluripotent ground state. *Cell* 2009, 138:722-737.
13. de Mello JCM, de Araujo ESS, Stabellini R, Fraga AM, de Souza JES, Sumita DR, Camargo AA, Pereira LV: Random X inactivation and extensive mosaicism in human placenta revealed by analysis of allele-specific gene expression along the X chromosome. *PloS one* 2010, 5:e10947.
14. Penaherrera M, Jiang R, Avila L, Yuen R, Brown C, Robinson W: Patterns of placental development evaluated by X chromosome inactivation profiling provide a basis to evaluate the origin of epigenetic variation. *Human reproduction* 2012, 27:1745-1753.
15. Hamada H, Okae H, Toh H, Chiba H, Hiura H, Shirane K, Sato T, Suyama M, Yaegashi N, Sasaki H: Allele-specific methylome and transcriptome analysis reveals widespread imprinting in the human placenta. *The American Journal of Human Genetics* 2016, 99:1045-1058.
16. Wegrzyn P, Faro C, Falcon O, Peralta C, Nicolaidis K: Placental volume measured by three-dimensional ultrasound at 11 to 13+ 6 weeks of gestation: relation to chromosomal defects. *Ultrasound in obstetrics & gynecology* 2005, 26:28-32.
17. Mathur A, Stekol L, Schatz D, MacLaren N, Scott M, Lippe B: The parental origin of the single X chromosome in Turner syndrome: lack of correlation with parental age or clinical phenotype. *American journal of human genetics* 1991, 48:682.
18. Jacobs P, Hassold T, Harvey J, May K: The origin of sex chromosome aneuploidy. *Progress in clinical and biological research* 1989, 311:135.
19. Álvarez-Nava F, Lanes R, Quintero JM, Miras M, Fideleff H, Mericq V, Marcato H, Zabala W, Soto M, Pardo T: Effect of the parental origin of the X-chromosome on the clinical features, associated complications, the two-year-response to growth hormone (rhGH) and the biochemical profile in patients with turner syndrome. *International journal of pediatric endocrinology* 2013, 2013:10.
20. Sagi L, Zuckerman-Levin N, Gawlik A, Ghizzoni L, Buyukgebiz A, Rakover Y, Bistritzer T, Admoni O, Vottero A, Baruch O: Clinical significance of the parental origin of the X chromosome in turner syndrome. *The Journal of Clinical Endocrinology & Metabolism* 2007, 92:846-852.
21. Ko JM, Kim JM, Kim GH, Lee BH, Yoo HW: Influence of parental origin of the X chromosome on physical

- phenotypes and GH responsiveness of patients with Turner syndrome. *Clinical endocrinology* 2010, 73:66-71.
22. Uematsu A, Yorifuji T, Muroi J, Kawai M, Mamada M, Kaji M, Yamanaka C, Momoi T, Nakahata T: Parental origin of normal X chromosomes in Turner syndrome patients with various karyotypes: implications for the mechanism leading to generation of a 45,X karyotype. *American journal of medical genetics* 2002, 111:134-139.
 23. Monroy N, López M, Cervantes A, García-Cruz D, Zafra G, Canún S, Zenteno JC, Kofman-Alfaro S: Microsatellite analysis in Turner syndrome: parental origin of X chromosomes and possible mechanism of formation of abnormal chromosomes. *American journal of medical genetics* 2002, 107:181-189.
 24. Jansson T: Placenta plays a critical role in maternal-fetal resource allocation. *Proc Natl Acad Sci U S A* 2016, 113:11066-11068.
 25. Coan PM, Conroy N, Burton GJ, Ferguson-Smith AC: Origin and characteristics of glycogen cells in the developing murine placenta. *Dev Dyn* 2006, 235:3280-3294.
 26. Adelman DM, Gertsenstein M, Nagy A, Simon MC, Maltepe E: Placental cell fates are regulated in vivo by HIF-mediated hypoxia responses. *Genes Dev* 2000, 14:3191-3203.
 27. Higgins JS, Vaughan OR, Fernandez de Liger E, Fowden AL, Sferruzzi-Perri AN: Placental phenotype and resource allocation to fetal growth are modified by the timing and degree of hypoxia during mouse pregnancy. *J Physiol* 2016, 594:1341-1356.
 28. Ganguly A, Collis L, Devaskar SU: Placental glucose and amino acid transport in calorie-restricted wild-type and Glut3 null heterozygous mice. *Endocrinology* 2012, 153:3995-4007.
 29. Fowden AL, Sferruzzi-Perri AN, Coan PM, Constanica M, Burton GJ: Placental efficiency and adaptation: endocrine regulation. *J Physiol* 2009, 587:3459-3472.
 30. Dimasuay KG, Boeuf P, Powell TL, Jansson T: Placental Responses to Changes in the Maternal Environment Determine Fetal Growth. *Front Physiol* 2016, 7:12.
 31. Hemberger M: The role of the X chromosome in mammalian extra embryonic development. *Cytogenet Genome Res* 2002, 99:210-217.
 32. Himes KP, Koppes E, Chaillet JR: Generalized disruption of inherited genomic imprints leads to wide-ranging placental defects and dysregulated fetal growth. *Dev Biol* 2013, 373:72-82.
 33. Lefebvre L: The placental imprintome and imprinted gene function in the trophoblast glycogen cell lineage. *Reprod Biomed Online* 2012, 25:44-57.
 34. Sandovici I, Hoelle K, Angiolini E, Constanica M: Placental adaptations to the maternal-fetal environment: implications for fetal growth and developmental programming. *Reprod Biomed Online* 2012, 25:68-89.
 35. Jamieson RV, Tan SS, Tam PP: Retarded postimplantation development of XO mouse embryos: impact of the parental origin of the monosomic X chromosome. *Dev Biol* 1998, 201:13-25.
 36. Zechner U, Reule M, Burgoyne PS, Schubert A, Orth A, Hameister H, Fundele R: Paternal transmission of X-linked placental dysplasia in mouse interspecific hybrids. *Genetics* 1997, 146:1399-1405.
 37. Ishikawa H, Rattigan A, Fundele R, Burgoyne PS: Effects of sex chromosome dosage on placental size in mice. *Biol Reprod* 2003, 69:483-488.
 38. de Melo Bernardo A, Heeren AM, van Iperen L, Fernandes MG, He N, Anjie S, Noce T, Ramos ES, de Sousa Lopes SM: Meiotic wave adds extra asymmetry to the development of female chicken gonads. *Mol Reprod Dev* 2015.
 39. María Emilia Solano KT, Mirka Katharina Kowal, Petra Clara Arck: Identification of suitable reference genes in the mouse placenta. *Placenta* 2016, 39:7-15.
 40. Heeren AM, van Iperen L, Klootwijk DB, de Melo Bernardo A, Roost MS, Gomes Fernandes MM, Louwe LA, Hilders CG, Helmerhorst FM, van der Westerlaken LA, Chuva de Sousa Lopes SM: Development of the follicular basement membrane during human gametogenesis and early folliculogenesis. *BMC Dev Biol* 2015, 15:4.
 41. Romijn HJ, van Uum JF, Emmering J, Goncharuk V, Buijs RM: Colocalization of VIP with AVP in neurons of the human paraventricular, supraoptic and suprachiasmatic nucleus. *Brain Res* 1999, 832:47-53.
 42. Zhao FQ, Keating AF: Functional properties and genomics of glucose transporters. *Curr Genomics* 2007, 8:113-128.

43. Tuttle S, Stamato T, Perez ML, Biaglow J: Glucose-6-phosphate dehydrogenase and the oxidative pentose phosphate cycle protect cells against apoptosis induced by low doses of ionizing radiation. *Radiat Res* 2000, 153:781-787.
44. Semenza GL, Roth PH, Fang HM, Wang GL: Transcriptional regulation of genes encoding glycolytic enzymes by hypoxia-inducible factor 1. *J Biol Chem* 1994, 269:23757-23763.
45. Davies W, Isles A, Smith R, Karunadasa D, Burrmann D, Humby T, Ojarikre O, Biggin C, Skuse D, Burgoyne P: Xlr3b is a new imprinted candidate for X-linked parent-of-origin effects on cognitive function in mice. *Nature genetics* 2005, 37:625-629.
46. Raefski AS, O'Neill MJ: Identification of a cluster of X-linked imprinted genes in mice. *Nature genetics* 2005, 37:620-624.
47. Thornhill AR, Burgoyne PS: A paternally imprinted X chromosome retards the development of the early mouse embryo. *Development* 1993, 118:171-174.
48. Harper MI, Fosten M, Monk M: Preferential paternal X inactivation in extraembryonic tissues of early mouse embryos. *J Embryol Exp Morphol* 1982, 67:127-135.
49. Coan PM, Ferguson-Smith AC, Burton GJ: Developmental dynamics of the definitive mouse placenta assessed by stereology. *Biol Reprod* 2004, 70:1806-1813.
50. Redline RW, Chernicky CL, Tan HQ, Ilan J, Ilan J: Differential expression of insulin-like growth factor-II in specific regions of the late (post day 9.5) murine placenta. *Molecular reproduction and development* 1993, 36:121-129.
51. Sibley C, Coan P, Ferguson-Smith A, Dean W, Hughes J, Smith P, Reik W, Burton G, Fowden A, Constancia M: Placental-specific insulin-like growth factor 2 (*Igf2*) regulates the diffusional exchange characteristics of the mouse placenta. *Proceedings of the National Academy of Sciences of the United States of America* 2004, 101:8204-8208.
52. Li Y, Behringer RR: *Esx1* is an X-chromosome-imprinted regulator of placental development and fetal growth. *Nature genetics* 1998, 20:309-311.
53. Withington S, Scott A, Saunders D, Floro KL, Preis J, Michalicek J, Maclean K, Sparrow D, Barbera JM, Dunwoodie S: Loss of *Cited2* affects trophoblast formation and vascularization of the mouse placenta. *Developmental biology* 2006, 294:67-82.
54. Lopez M, Dikkes P, Zurakowski D, Villa-Komaroff L: Insulin-like growth factor II affects the appearance and glycogen content of glycogen cells in the murine placenta. *Endocrinology* 1996, 137:2100-2108.
55. Takahashi K, Kobayashi T, Kanayama N: *p57Kip2* regulates the proper development of labyrinthine and spongiotrophoblasts. *Molecular human reproduction* 2000, 6:1019-1025.
56. Sood R, Kalloway S, Mast AE, Hillard CJ, Weiler H: Fetomaternal cross talk in the placental vascular bed: control of coagulation by trophoblast cells. *Blood* 2006, 107:3173-3180.
57. Redecha P, van Rooijen N, Torry D, Girardi G: Pravastatin prevents miscarriages in mice: role of tissue factor in placental and fetal injury. *Blood* 2009, 113:4101-4109.
58. Vogt E, Ng A-K, Rote NS: A model for the antiphospholipid antibody syndrome: monoclonal antiphosphatidylserine antibody induces intrauterine growth restriction in mice. *American journal of obstetrics and gynecology* 1996, 174:700-707.
59. Nelson DM, Crouch EC, Curran EM, Farmer DR: Trophoblast interaction with fibrin matrix. Epithelialization of perivillous fibrin deposits as a mechanism for villous repair in the human placenta. *Am J Pathol* 1990, 136:855-865.
60. Khan HM, Khan MY, Minhas LA: Histological study of the developing mouse placenta. *Journal of Rawalpindi Medical College* 2011, 15:116-119.
61. Gu J-M, Crawley JT, Ferrell G, Zhang F, Li W, Esmon NL, Esmon CT: Disruption of the endothelial cell protein C receptor gene in mice causes placental thrombosis and early embryonic lethality. *Journal of Biological Chemistry* 2002, 277:43335-43343.
62. Monkley SJ, Delaney SJ, Pennisi DJ, Christiansen JH, Wainwright BJ: Targeted disruption of the *Wnt2* gene results in placentation defects. *DEVELOPMENT-CAMBRIDGE-* 1996, 122:3343-3353.



